Deformation effect on the double Gamow-Teller matrix element of ^{100}Mo for the $0^+ \rightarrow 0^+$ transition

B. M. Dixit and P. K. Rath
Department of Physics, Lucknow University, Lucknow-226 007, India

P. K. Raina
Department of Physics and Meteorology, Indian Institute of Technology, Kharagpur-721 302, India
(Received 16 May 2001; published 21 February 2002)

The two neutrino double beta decay of ^{100}Mo for the $0^+ \rightarrow 0^+$ transition is studied in the Hartree-Fock-Bogoliubov (HFB) framework. Prior to the calculation of the double Gamow-Teller matrix element $M_{\mathrm{GT}}^{2\nu}$, the reliability of the intrinsic wave functions has been established by obtaining an overall agreement between a number of theoretically calculated spectroscopic properties and the available experimental data for ^{100}Mo and ^{100}Ru. It has been further noticed that there is a necessity of an appropriate amount of deformation in the HFB intrinsic state to obtain a realistic $M_{\mathrm{GT}}^{2\nu}$.

DOI: 10.1103/PhysRevC.65.034311 PACS number(s): 23.40.Hc, 21.60.Jz, 23.20.−g, 27.60.+j

I. INTRODUCTION

The nuclear double beta decay is expected to proceed through two different modes, namely, the two neutrino double beta ($2\nu\beta\beta$) decay and the neutrinoless double beta ($0\nu\beta\beta$) decay. Historically the former was studied by Mayer in 1935 [1] to account for the stability of some even Z-even N nuclei which are otherwise candidates for beta decay and the latter was conjectured by Fury [2] assuming the electron neutrino to be a Majorana particle [3]. The implications of present studies about nuclear $\beta\beta$ decay are far reaching in nature. The nuclear $\beta\beta$ decay in general and $0\nu\beta\beta$ decay in particular is a convenient tool to test the physics beyond the standard model (SM) [4]. These aspects of nuclear $\beta\beta$ decay have been excellently reviewed in detail over the past years [5–16].

The $2\nu\beta\beta$ decay, which is a second order process of weak interaction and conserves the lepton number exactly, is allowed in the SM. The half-life of $2\nu\beta\beta$ decay is a product of an accurately known phase space factor and an appropriate nuclear transition matrix element $M_{2\nu}$. As the half-lives of $2\nu\beta\beta$ decay have been already measured for about ten nuclei, the values of the $M_{2\nu}$ matrix element can be extracted directly. Consequently, the validity of different models employed for nuclear structure calculations can be tested by calculating the $M_{2\nu}$. The $0\nu\beta\beta$ decay is not observed so far. Hence the models predict the half-lives assuming a certain value for the neutrino mass or conversely extract various parameters from the observed limits of the half-lives of $0\nu\beta\beta$ decay. The reliability of predictions can be judged *a priori* only from the success of a nuclear model in explaining various observed physical properties of nuclei. The common practice is to calculate the $M_{2\nu}$ to start with and compare with the experimentally observed value as the two decay modes involve the same set of initial and final nuclear wave functions.

It is observed that in all cases the $2\nu\beta\beta$ decay matrix elements $M_{2\nu}$ are sufficiently quenched. The main motive for all theoretical calculations is to understand the physical mechanism responsible for the suppression of the $M_{2\nu}$. Over the past few years, several nuclear models have been employed to calculate the $2\nu\beta\beta$ decay transition matrix elements in a two-nucleon ($2n$) mechanism. The $M_{2\nu}$ is calculated mainly in three types of models. One is the shell model and its variants. The second is the quasiparticle random phase approximation (QRPA) and extensions thereof. The third type of model is classified as alternative models. The details about these models—their advantages as well as shortcomings—have been discussed excellently by Suhonen and Civitarese [14] and Faessler and Simkovic [15] in the recent past. For the sake of completeness, we briefly discuss below the relative applicability, success, and failure of various models used so far to study the $\beta\beta$ decay process.

The shell model, which attempts to solve the nuclear many-body problem as exactly as possible, is the best choice for the calculation of the $M_{2\nu}$. Beyond the pf shell, the number of basis states increases so drastically that a few years back it was not possible to perform a conventional shell model calculation without imposing a certain truncation scheme. On the other hand, most of the $\beta\beta$ decay emitters are medium or heavy mass nuclei. As a reliable shell model calculation was difficult to perform, Haxton and Stephenson [7] and Vergados [9] have studied the $\beta\beta$ decay of ^{76}Ge, ^{82}Se, and ^{128,130}Te nuclei in the weak coupling limit. Recent large scale shell model calculations are more promising in nature [17–20]. The calculations by Caurier *et al.* [19] are more realistic in nature; the $M_{2\nu}$ of ^{82}Se is calculated exactly and those of ^{76}Ge and ^{136}Xe are dealt with in a nearly exact manner. The conventional shell model and Monte Carlo shell model (MCSM) [21,22] have been tested against each other for the case of ^{48}Ca and ^{76}Ge and the agreement is interestingly good. Hence the MCSM could be a good alternative to conventional shell model calculations in the near future.

Vogel and Zirnbauer were the first to provide an understanding of the observed suppression of $M_{2\nu}$ in the QRPA model [23]. In $\beta\beta$ decay, the initial nucleus decays into the final nucleus through the virtual excitation of all possible states of the intermediate odd-odd nucleus. The proton-neutron particle-hole (p-h) or proton-neutron particle-particle (p-p) interaction matrix elements are required to calculate the excited states of the intermediate nucleus. The

p-h and p-p interactions are responsible for the concentration of the Gamow-Teller (GT) strength in the giant GT resonance and the reduction of total β^+ strength, respectively. The p-p interaction has negligible effect on the strength of the giant GT resonance and was usually neglected. It was observed that the quenching of $M_{2\nu}$ can be achieved by a proper inclusion of ground state correlations through the p-p interaction in the $S=1$, $T=0$ channel and the calculated half-lives are in close agreement with all the experimental data [23]. The QRPA frequently overestimates the ground state correlations as a result of an increase in the strength of attractive proton-neutron interaction leading to the collapse of QRPA solutions. The physical value of this force is usually close to the point at which the QRPA solutions collapse. To cure the strong suppression of $M_{2\nu}$, several extensions of the QRPA have been proposed. The most important proposals are inclusion of proton-neutron pairing, higher QRPA, particle number projection, the multiple commutator method (MCM), and renormalized QRPA. However none of the above methods is free from ambiguities [15]. Similarly under alternative models, the operator expansion method (OEM), the broken SU(4) symmetry, the pseudo-SU(3), and the single state dominance model have their own problems [14].

A large number of theoretical as well as experimental studies of the $2\nu\beta\beta$ decay have been already done for ^{100}Mo over the past few years. In Table III below, we have presented a summary of all the available experimental [24–30] and theoretical [14,31–38] results. Experimental studies involving in-beam γ-ray spectroscopy have yielded a vast amount of data concerning the level energies as well as electromagnetic properties over the past years. Thus the $\beta\beta$ decay is not an isolated nuclear process. Although the availability of data permits a rigorous and detailed critique of the ingredients of the microscopic framework that seeks to provide a description of these isotopes, most of the calculations of $\beta\beta$ decay matrix elements performed so far do not satisfy this criterion.

The structure of nuclei in the mass region $A=100$ involving Mo and Ru isotopes is quite complex. With the discovery of a new region of deformation around $A=100$ by Cheifetz *et al.* [39], a well developed rotational spectra was observed in several neutron-rich Mo and Ru isotopes during a study of fission fragments of ^{252}Cf. The $B(E2,\ 0^+\rightarrow 2^+)$ values were observed to be as enhanced as in the rare-earth and actinide regions. This mass region offered a nice example of shape transition that is the sudden onset of deformation at neutron number $N=60$. The nuclei are soft vibrators for neutron number $N<60$ and quasirotors for $N>60$. The nuclei with neutron number $N=60$ are transitional nuclei. All the nuclei undergoing $\beta\beta$ decay are even-even type, in which the pairing degrees of freedom play an important role. Moreover, it has been already conjectured that the deformation can play a crucial role in the case of $\beta\beta$ decay of ^{100}Mo and ^{150}Nd [35,36]. Hence it is desirable to have a model which incorporates the pairing and deformation degrees of freedom on equal footing in its formalism. For this purpose, the projected Hartree-Fock-Bogoliubov (PHFB) model is one of the most natural choices. However in the PHFB model, the double Gamow-Teller (DGT) matrix element $M^{2\nu}_{\rm GT}$ has to be calculated using the closure approximation. The closure approximation, which is used to simplify the numerical calculation avoiding the explicit construction of intermediate states, estimates some average excitation energy $\langle E_N\rangle$ for the intermediate states. The validity of this approximation for $2\nu\beta\beta$ decay is ambiguous while for $0\nu\beta\beta$ decay it is quite good. This approximation has been shown to work badly in the case where the $M^{2\nu}_{\rm GT}$ are predominantly of one sign for some lower $\langle E_N\rangle$ and of opposite sign for a larger $\langle E_N\rangle$. It is therefore better to avoid the closure approximation whenever possible [40,41]. Hence there is no *a priori* justification against the closure approximation. The validity of the closure approximation is to be decided *a posteriori* by comparing the theoretically calculated and experimentally extracted $M_{2\nu}$.

Over the past 15 years, extensive studies of shape transition vis-à-vis electromagnetic properties of Zr and Mo isotopes [42–44] have been successfully carried out in the PHFB framework using the pairing plus quadrupole-quadrupole (PPQQ) interaction. The success of the PHFB model in explaining the observed experimental trends in the mass region $A=100$ has motivated us to apply the PHFB wave functions to study the nuclear $\beta\beta$ decay transition $^{100}\mathrm{Mo}\rightarrow{}^{100}\mathrm{Ru}$. It is well known that the pairing part of the two-body interaction is responsible for the reduction of collectivity whereas the quadrupole-quadrupole (QQ) interaction enhances the collectivity in the nuclear intrinsic wave functions. In other words the pairing interaction is responsible for the sphericity of the nucleus whereas the QQ interaction makes the nucleus deformed. Hence to examine the explicit role of deformation degrees of freedom vis-à-vis the suppression of $M^{2\nu}_{\rm GT}$, the PPQQ interaction will be the most appropriate choice.

To summarize, our aim is to study the $2\nu\beta\beta$ decay not isolatedly but together with other observed nuclear phenomena. This is in accordance with the basic philosophy of nuclear many-body theory, which is to explain all the observed properties of nuclei in a coherent manner. Hence as a test of the reliability of the wave functions, we have calculated the yrast spectra, reduced $B(E2)$ transition probabilities, static quadrupole moments, and g factors of ^{100}Mo and ^{100}Ru nuclei and compared these with the available experimental data. Subsequently the HFB wave functions of ^{100}Mo and ^{100}Ru are employed to calculate the $M^{2\nu}_{\rm GT}$. We have also studied the role of deformation on $M^{2\nu}_{\rm GT}$ through varying single particle field and strength of the QQ interaction. This paper is organized as follows. In Sec. II, we present the theoretical formalism briefly. The results are presented and discussed in Sec. III. The conclusions are finally given in Sec. IV.

II. CALCULATIONAL FRAMEWORK

The theoretical formalism to calculate the half-life of the $2\nu\beta\beta$ decay mode has been given by Haxton and Stephenson [7], Doi *et al.* [8], and Tomoda [11]. Hence in Sec. II A, we briefly outline steps of the above derivations for clarity in notations used in the present paper. We have given

expressions to calculate the nuclear spectroscopic properties, namely, yrast spectra, reduced $B(E2)$ transition probabilities, static quadrupole moments [44], and g factors [45] in Sec. II B. Further, in Sec. II C, we have presented formulas to calculate the nuclear transition matrix elements of the $\beta\beta$ decay in the PHFB model [46].

A. The $0^+\rightarrow 0^+$ transition of the $2\nu\beta\beta$ decay mode

The effective weak interaction Hamiltonian density for beta decay due to W-boson exchange is assumed to be

$$H_W=\frac{G}{\sqrt{2}}(j_{L\mu}J_L^{\mu\dagger}+\kappa j_{L\mu}J_R^{\mu\dagger}+\eta j_{R\mu}J_L^{\mu\dagger}+\lambda j_{R\mu}J_R^{\mu\dagger})+\text{H.c.} \tag{2.1}$$

We use $G=1.166\,37\times 10^{-5}$ GeV^{-2}. The coupling constants κ, η, and λ are small parameters ($\ll 1$). The left and right handed weak leptonic charged currents are given by $V\pm A$ forms,

$$j_L^{\mu}=\bar{e}\gamma^{\mu}(1-\gamma_5)\nu_{eL}, \quad j_R^{\mu}=\bar{e}\gamma^{\mu}(1+\gamma_5)\nu'_{eR}, \tag{2.2}$$

where

$$\nu_{eL}=\sum_{i=1}^{2n} U_{ei}N_{iL}, \quad \nu'_{eR}=\sum_{i=1}^{2n} V_{ei}N_{iR}. \tag{2.3}$$

Here N_i is a Majorana neutrino field with mass m_i. In Eq. (2.3), a Dirac neutrino is expressed as a superposition of a pair of mass degenerate Majorana neutrinos in the most general form. Further the mixing parameters are constrained by the following orthonormality conditions:

$$\sum_j |U_{ej}|^2=\sum_j |V_{ej}|^2=1, \quad \sum_j U_{ej}V_{ej}=0. \tag{2.4}$$

In the nonrelativistic impulse approximation, the left and right handed hadronic currents for nuclear beta decay in $V\pm A$ forms are given by

$$J_L^{\mu\dagger}(x)=\sum_{n=1}^{A}\tau_n^+\,\delta(\mathbf{x}-\mathbf{r}_n)[(g_V-g_AC_n)g^{\mu 0}+(g_A\sigma_n^k-g_VD_n^k)g^{\mu k}], \tag{2.5a}$$

$$J_R^{\mu\dagger}(x)=\sum_{n=1}^{A}\tau_n^+\,\delta(\mathbf{x}-\mathbf{r}_n)[(g_V+g_AC_n)g^{\mu 0}+(-g_A\sigma_n^k-g_VD_n^k)g^{\mu k}]. \tag{2.5b}$$

The nuclear recoil terms C_n and $\mathbf{D}_n$ are defined as follows:

$$C_n=[(\mathbf{P}_n+\mathbf{P}'_n)\cdot\boldsymbol{\sigma}_n-(g_p/g_A)(E_n-E'_n)\boldsymbol{\sigma}_n\cdot\mathbf{Q}_n]/2M, \tag{2.6}$$

$$\mathbf{D}_n=[(\mathbf{P}_n+\mathbf{P}'_n)-i[1-2M(g_W/g_V)]\boldsymbol{\sigma}_n\times\mathbf{Q}_n]/2M, \tag{2.7}$$

where $\mathbf{Q}_n=\mathbf{P}_n-\mathbf{P}'_n$. g_V, g_A, g_P, and g_W are vector, axial vector, pseudoscalar, and weak magnetism terms. At $q^2=0$, $g_V(0)=1$, $g_A(0)=1.254$, and $g_P/g_A=2M_p/m_\pi^2$, where M_P and m_π are the proton and pion masses. By the conserved vector current hypothesis $g_W(0)=\kappa_\beta/2M$ and $\kappa_\beta=3.70$, where M and κ_β are the mass and isovector anomalous magnetic moment of nucleons, respectively. In the case of $2\nu\beta\beta$ decay, the recoil terms are usually neglected.

The $2\nu\beta\beta$ decay is a second order process in the effective weak interaction and takes place within the standard model of electroweak unification. Therefore the processes, which involve left handed currents only, give the dominant contribution. The following assumptions are made in deriving the $2\nu\beta\beta$ decay rate formula.

(i) Only light neutrino species are considered. Hence the normalization condition for the left handed neutrinos given by Eq. (2.4) can be rewritten as

$$\sum_{i,j}{}' |U_{ei}U_{ej}|^2\approx 1. \tag{2.8}$$

Again we assume that masses of these light neutrinos are much smaller than $Q_{\beta\beta}$, where

$$Q_{\beta\beta}=M_I-M_F-2m_e. \tag{2.9}$$

(ii) The S-wave state of the electron and the neutrino wave functions are retained. The total angular momentum of four S-wave leptons can be 0, 1, or 2 and is equal to the total angular momentum transferred from the nucleus. However, we restrict ourselves to the $0^+\rightarrow 0^+$ transition only and hence retain the dominant terms **1** and $\boldsymbol{\sigma}$ in the nuclear currents.

(iii) The final nucleus and the initial nucleus differ by two units of isospin for any $\beta\beta$ decay of practical interest. The contributions of the successive Fermi transitions can be safely neglected as they come from isospin mixing effects. The half-life of the $2\nu\beta\beta$ decay for the $0^+\rightarrow 0^+$ transition is given by

$$[T_{1/2}^{2\nu}(0^+\rightarrow 0^+)]^{-1}=G_{2\nu}|M_{2\nu}|^2, \tag{2.10}$$

where

$$M^{2\nu}=\sum_N \frac{\langle 0^+||\boldsymbol{\sigma}\tau^+||1_N^+\rangle\langle 1_N^+||\boldsymbol{\sigma}\tau^+||0^+\rangle}{E_N-(M_I+M_F)/2} \tag{2.11}$$

and the integrated kinematical factor $G_{2\nu}$ can be calculated with good accuracy [8].

(iv) If the E_N of Eq. (2.11) is replaced by an average $\langle E_N\rangle$, the summation over intermediate states can be completed using the closure approximation and one obtains

$$M_{2\nu}=-\frac{2M_{\rm GT}^{2\nu}}{\langle E_N\rangle-(M_I+M_F)/2}=-\frac{2M_{\rm GT}^{2\nu}}{E_d}, \tag{2.12}$$

where the DGT matrix element $M_{\rm GT}^{2\nu}$ is defined as follows:

$$M_{\rm GT}^{2\nu}=\frac{1}{2}\langle 0^+|\sum_{n,m}\boldsymbol{\sigma}_n\cdot\boldsymbol{\sigma}_m\tau_n^+\tau_m^+|0^+\rangle \tag{2.13}$$

and

$$E_d = \langle E_N \rangle - (M_I + M_F)/2 = \frac{1}{2} W_0 + \langle E_N \rangle - M_I . \tag{2.14}$$

Here W_0 is the total released energy and is given by $W_0 = M_I - M_F = Q_{\beta\beta} + 2m_e$.

B. Spectroscopic properties of yrast states

The procedure for obtaining the HFB intrinsic states has been discussed by Goodman [47]. The axially symmetric HFB intrinsic state with $K=0$ can be written as

$$|\Phi_0\rangle = \Pi_{im}(U_{im} + V_{im} b^\dagger_{im} b^\dagger_{\bar{i}m})|0\rangle, \tag{2.15}$$

where the creation operators $b^\dagger_{im}$ and $b^\dagger_{\bar{i}m}$ are given by

$$b^\dagger_{im} = \sum_\alpha c_{i\alpha,m} a^\dagger_{\alpha m}, \quad b^\dagger_{\bar{i}m} = \sum_\alpha (-1)^{l+j-m} c_{i\alpha,m} a^\dagger_{\alpha,-m}. \tag{2.16}$$

Using the standard projection technique [48], a state with good angular momentum is obtained from the HFB intrinsic state through the following relation:

$$|\Psi^J_{MK}\rangle = P^J_{MK}|\Phi_K\rangle = \left[\frac{(2J+1)}{8\pi^2}\right] \int D^J_{MK}(\Omega) R(\Omega) |\Phi_K\rangle d\Omega, \tag{2.17}$$

where $R(\Omega)$ and $D^J_{MK}(\Omega)$ are the rotation operator and the rotation matrix, respectively. Expressions used to calculate (1) yrast spectra, (2) reduced transition probabilities $BE(2)$ and static quadrupole moments $Q(J^\pi)$ [44], and (3) g factors [45] are given in the following subsections.

1. Yrast spectra

The energy E_J of a state with angular momentum J can be written as

$$E_J = \frac{\langle \Phi_0 | H P^J_{00} | \Phi_0 \rangle}{\langle \Phi_0 | P^J_{00} | \Phi_0 \rangle} = \frac{\int_0^\pi h(\theta) n(\theta) d^J_{00}(\theta) \sin\theta d\theta}{\int_0^\pi n(\theta) d^J_{00}(\theta) \sin\theta d\theta}, \tag{2.18}$$

where the two-body Hamiltonian H is given by

$$H = \sum_\alpha \epsilon_\alpha a^\dagger_\alpha a_\alpha + \frac{1}{4} \sum_{\alpha\beta\gamma\delta} \langle \alpha\beta | V | \gamma\delta \rangle a^\dagger_\alpha a^\dagger_\beta a_\delta a_\gamma \tag{2.19}$$

and

$$h(\theta) = \sum_\alpha \epsilon_\alpha \left(\frac{M}{1+M}\right)_{\alpha\alpha} + \frac{1}{4} \sum_{\alpha\beta\gamma\delta} \langle \alpha\beta | V | \gamma\delta \rangle \times \left\{ 2 \left(\frac{M}{1+M}\right)_{\gamma\alpha} \left(\frac{M}{1+M}\right)_{\delta\beta} + \sum_{\nu\rho} \left(\frac{M}{1+M}\right)_{\gamma\rho} F_{\rho\delta} \left(\frac{M}{1+M}\right)_{\nu\alpha} f_{\nu\beta} \right\}, \tag{2.20}$$

$$n(\theta) = \sqrt{\det[1 + M(\theta)]}, \tag{2.21}$$

$$M(\theta) = F_{\alpha\beta}(\theta) f^\dagger_{\alpha\beta}, \tag{2.22}$$

$$F_{\alpha\beta}(\theta) = \sum_{m'_\alpha m'_\beta} d^{j_\alpha}_{m_\alpha, m'_\alpha}(\theta) d^{j_\beta}_{m_\beta, m'_\beta}(\theta) f_{j_\alpha m'_\alpha, j_\beta m'_\beta}, \tag{2.23}$$

$$f_{\alpha\beta} = \sum_i c_{ij_\alpha, m_\alpha} c_{ij_\beta, m_\beta} (V_{im_\alpha}/U_{im_\alpha}) \delta_{m_\alpha, -m_\beta}. \tag{2.24}$$

2. Transition probabilities $BE(2)$ and static quadrupole moments $Q(J^\pi)$

Employing the angular momentum projected wave function $|\Psi^J_K\rangle$, one obtains the following expression for reduced transition probability $B(E2)$:

$$B(E2: J_i \to J_f) = \left(\frac{5}{16\pi}\right) (e_\pi \langle Q^2_0 \rangle_\pi + e_\nu \langle Q^2_0 \rangle_\nu)^2, \tag{2.25}$$

where

$$\langle Q^2_0 \rangle_{\tau_3} = \langle \Psi^{J_i}_K | Q^2_0 | \Psi^{J_f}_K \rangle = [n^{J_i} n^{J_f}]^{-1/2} \int_0^\pi \sum_\mu \begin{pmatrix} J_i & 2 & J_f \\ -\mu & \mu & 0 \end{pmatrix} d^{J_i}_{-\mu 0}(\theta) n(\theta) \times \left[b^2 \sum_{\tau_3 \alpha\beta} e_{\tau_3} \langle \alpha | Q^2_\mu | \beta \rangle \rho^{\tau_3}_{\alpha\beta}(\theta) \right] \sin\theta d\theta, \tag{2.26}$$

$$n^J = \int_0^\pi n(\theta) d^J_{00}(\theta) \sin\theta d\theta, \tag{2.27}$$

$$\rho^{\tau_3}_{\alpha\beta}(\theta) = \{ M(\theta)/[1 + M(\theta)] \}^{\tau_3}_{\alpha\beta}, \tag{2.28}$$

and

$$Q^2_\mu = \sqrt{\frac{16\pi}{5}} \frac{r^2}{b^2} Y^2_\mu(\theta, \phi). \tag{2.29}$$

Similarly the static quadrupole moments $Q(J^\pi)$ are evaluated using the expression

$$Q(J^\pi)=\langle\Psi_K^J|Q_0^2|\Psi_K^J\rangle$$
$$=[n^J]^{-1}\begin{pmatrix} J & 2 & J \\ J & 0 & J\end{pmatrix}\int_0^\pi\sum_\mu\begin{pmatrix} J & 2 & J \\ -\mu & \mu & 0\end{pmatrix}$$
$$\times d^J_{-\mu 0}(\theta)n(\theta)$$
$$\times\left[b^2\sum_{\tau_3\alpha\beta}e_{\tau_3}\langle\alpha|Q_\mu^2|\beta\rangle\rho^{\tau_3}_{\alpha\beta}(\theta)\right]\sin\theta d\theta. \tag{2.30}$$

3. g factors

The expression for obtaining g factors of yrast states is given by

$$g(J^\pi)=\frac{\langle\Psi^J_{00}|\mu_z|\Psi^J_{00}\rangle}{J}$$
$$=(n^JJ)^{-1}\int_0^\pi n(\theta)\sum_m\begin{pmatrix} J & 1 & J \\ -m & m & 0\end{pmatrix}$$
$$\times d^J_{-m0}(\theta)\sum_{\tau_3\alpha\beta}\langle\alpha|\mu_m|\beta\rangle\rho^{\tau_3}_{\alpha\beta}(\theta)\sin\theta d\theta, \tag{2.31}$$

where in general

$$\boldsymbol{\mu}=g_l'\mathbf{l}+g_s'\mathbf{s}+g_p(Y^{(2)}\times S^{(2)})^{(1)}. \tag{2.32}$$

Here g_l' ,(g_s') are the effective orbital (spin) g factors and g_p provides a measure of the spin-polarization effects. In the present calculation we have neglected the contributions of spin-polarization effects.

C. Nuclear transition matrix elements in the PHFB framework

In the closure approximation, the relevant transition operators responsible for the $\beta\beta$ decay are two-body operators and in general are given by

$$O_{\alpha\beta\gamma\delta}=\frac{1}{4}\sum_{\alpha\beta\gamma\delta}\langle\alpha\beta|V|\gamma\delta\rangle a^\dagger_\alpha a^\dagger_\beta a_\delta a_\gamma. \tag{2.33}$$

Employing the HFB wave functions, one obtains the following expression for the double beta decay nuclear transition matrix elements [46]:

$$\langle O\rangle=[n^{J_f=0}n^{J_i=0}]^{-1/2}\int_0^\pi n_{(N,Z),(N-2,Z+2)}$$
$$\times(\theta)\frac{1}{4}\sum_{\alpha\beta\gamma\delta}\langle O_{\alpha\beta\gamma\delta}\rangle\sum_{\epsilon\eta}[(1+F^{(\pi)}_{N,Z}(\theta)f^{(\pi)}_{N-2,Z+2})]^{-1}_{\epsilon\alpha}$$
$$\times(f^{(\pi)}_{N-2,Z+2})_{\epsilon\beta}[(1+F^{(\nu)}_{N,Z}(\theta)f^{(\nu)}_{N-2,Z+2})]^{-1}_{\gamma\eta}$$
$$\times(F^{(\nu)}_{N,Z})^{-1}_{\eta\delta}\sin\theta d\theta, \tag{2.34}$$

where

$$n^J=\int_0^\pi[\det(1+F^{(\pi)}f^{(\pi)^\dagger})]^{1/2}$$
$$\times[\det(1+F^{(\nu)}f^{(\nu)^\dagger})]^{1/2}d^J_{00}(\theta)\sin(\theta)d\theta \tag{2.35}$$

and

$$n_{(N,Z),(N-2,Z+2)}(\theta)=[\det(1+F^{(\nu)}_{N,Z}f^{(\nu)^\dagger}_{N-2,Z+2})]^{1/2}$$
$$\times[\det(1+F^{(\pi)}_{N,Z}f^{(\pi)^\dagger}_{N-2,Z+2})]^{1/2}. \tag{2.36}$$

The $\pi(\nu)$ represents the proton (neutron) of nuclei involved in the double beta decay process. The matrices for $[F_{N,Z}(\theta)]_{\alpha\beta}$ and $[f_{N,Z}(\theta)]_{\alpha\beta}$ are given by Eqs. (2.23) and (2.24) The required nuclear transition matrix elements are calculated in the following manner. We use the results of PHFB calculations which are summarized by the amplitudes (U_{im},V_{im}) and the expansion coefficient $c_{ij,m}$. In the first step matrices $F^{(\pi,\nu)}$ and $f^{(\pi,\nu)}$ are set up for the nuclei involved in the double beta decay making use of 20 Gaussian quadrature points in the range $(0,\pi)$. Finally using Eq. (2.34), the required nuclear transition matrix elements can be calculated in a straightforward manner.

III. RESULTS AND DISCUSSIONS

A. The one- and two-body parts of the Hamiltonian

In the present calculations we have treated the doubly even shell nucleus ^{76}Sr ($Z=N=38$) as an inert core, with the valence space spanned by the orbits $1p_{1/2}$, $2s_{1/2}$, $1d_{3/2}$, $1d_{5/2}$, $0g_{7/2}$, $0g_{9/2}$, and $0h_{11/2}$ for protons and neutrons. The orbit $1p_{1/2}$ has been included in the valence space to examine the role of the $Z=40$ proton core vis-à-vis the onset of deformation in the highly neutron-rich isotopes. The set of single particle energies (SPE's) used here are (in MeV) $\epsilon(1p_{1/2})=-0.8$, $\epsilon(0g_{9/2})=0.0$, $\epsilon(1d_{5/2})=5.4$, $\epsilon(2s_{1/2})=6.4$, $\epsilon(1d_{3/2})=7.9$, $\epsilon(0g_{7/2})=8.4$, and $\epsilon(0h_{11/2})=8.6$. This set of SPE's, but for the $\epsilon(0h_{11/2})$ which is slightly lowered, has been employed in a number of successful shell model [49,50] as well as variational model [42–44] calculations for nuclear properties in the mass region $A=100$.

The effective two-body interaction that has been used in the present calculation is the PPQQ type [51]. Explicitly the Hamiltonian can be written as

$$H=H_{sp}+V(P)+\chi_{qq}V(QQ). \tag{3.1}$$

The χ_{qq} is an arbitrary parameter and it has been introduced to study the role of deformation by varying the strength of QQ interaction. The final results are obtained by setting the $\chi_{qq}=1$ in the Hamiltonian given by Eq. (3.1). The pairing part of the effective interaction is written as

$$V(P)=-\left(\frac{G}{4}\right)\sum_{\alpha\beta}S_\alpha S_\beta a^\dagger_\alpha a^\dagger_{\bar\alpha}a_{\bar\beta}a_\beta, \tag{3.2}$$

TABLE I. Variation in excitation energies (in MeV) of $J^{\pi}=2^{+}$, 4^{+}, and 6^{+} yrast states of ^{100}Mo and ^{100}Ru nuclei with change in χ_{pn}, keeping fixed $G_P=-0.30$ MeV, $G_n=-0.20$ MeV, and $\epsilon(0h_{11/2})=8.6$ MeV.

Nucleus		χ_{pn} -0.0178	-0.0182	-0.0186	-0.0190	-0.0194	Experiment[a]
^{100}Mo	$\langle Q_0^2\rangle$	43.28	45.08	46.78	48.92	50.34	
	E_{2^+}	0.8406	0.6967	0.5904	0.5434	0.4565	0.5355
	E_{4^+}	1.9356	1.7104	1.5416	1.4843	1.3175	1.1359
	E_{6^+}	3.2101	2.9355	2.7314	2.6876	2.4645	
^{100}Ru	$\langle Q_0^2\rangle$	44.76	45.40	46.00	46.69	47.39	
	E_{2^+}	0.6152	0.5628	0.5138	0.4823	0.3172	0.5396
	E_{4^+}	1.7223	1.6087	1.5006	1.4306	1.0167	1.2265
	E_{6^+}	3.1337	2.9654	2.8049	2.7015	2.0398	2.0777

[a]Reference [56].

where α denotes the quantum numbers $(nljm)$. The state $\overline{\alpha}$ is same as α but with the sign of m reversed and S_i is the phase factor $(-1)^{j_i-m_i}$. The QQ part of the effective interaction is given by

$$V(QQ)=-\left(\frac{\chi}{2}\right)\sum_{\alpha\beta\gamma\delta}\sum_{\mu}(-1)^{\mu}\langle\alpha|q_{\mu}^{2}|\gamma\rangle \times\langle\beta|q_{-\mu}^{2}|\delta\rangle a_{\alpha}^{\dagger}a_{\beta}^{\dagger}a_{\delta}a_{\gamma}, \tag{3.3}$$

where

$$q_{\mu}^{2}=\left(\frac{16\pi}{5}\right)^{1/2}r^{2}Y_{\mu}^{2}(\theta,\phi). \tag{3.4}$$

The strength of the pairing interaction was fixed through the relation $G_p=-30/A$ MeV and $G_n=-20/A$ MeV. These values of G_p and G_n have been used by Heestand *et al.* [52] to successfully explain the experimental $g(2^+)$ data of some even-even Ge, Se, Mo, Ru, Pd, Cd, and Te isotopes in Greiner's collective model [53]. The strengths of the like-particle components of the QQ interaction are taken as $\chi_{pp}=\chi_{nn}=-0.0105$ MeV b^{-4}. The strength of the proton-neutron (pn) component of the QQ interaction χ_{pn} has been fixed to be -0.0190 and -0.0186 MeV b^{-4} for ^{100}Mo and ^{100}Ru, respectively, where b is an oscillator parameter. These values for the strength of the QQ interaction are comparable to those suggested by Arima on the basis of an empirical analysis of the effective two-body interactions [54].

B. The yrast spectra and electromagnetic properties

The χ_{pn} is varied so as to obtain the spectra of ^{100}Mo and ^{100}Ru in optimum agreement with the experimental results.

TABLE II. Comparison of the calculated and experimentally observed reduced transition probabilities $B(E2{:}0^+\rightarrow 2^+)$, static quadrupole moments $Q(2^+)$, and g factors $g(2^+)$. Here $B(E2)$ and $Q(2^+)$ are calculated in units of 10^{-50} e^2 cm^4 and e fm^2, respectively, for effective charge $e_p=1+e_{eff}$ and $e_n=e_{eff}$. The $g(2^+)$ has been calculated in units of nanometers for $g_l^{\pi}=1.0$, $g_l^{\nu}=0.0$, and $g_s^{\pi}=g_s^{\nu}=0.60$.

Nucleus	$B(E2{:}0^+\rightarrow 2^+)$ Theory e_{eff} 0.55	0.60	0.65	Experiment	$Q(2^+)$ Theory e_{eff} 0.55	0.60	0.65	Experiment[a]	$g(2^+)$ Theory	Experiment
^{100}Mo	45.7	50.9	56.5	47.0 ± 2.4[b] 51.1 ± 0.9[c] 34.0[d] 51.6 ± 1.0[e]	-0.61	-0.65	-0.68	-0.42 ± 0.09 -0.39 ± 0.08	0.471	0.34 ± 0.18[a]
^{100}Ru	44.7	49.7	54.9	53.1[d] 50.1 ± 1.0[e] 48.2 ± 2.6[g] 49.3 ± 0.3[h]	-0.61	-0.64	-0.67	-0.43 ± 0.07 -0.40 ± 0.12 -0.54 ± 0.07	0.357	0.42 ± 0.03[a] 0.47 ± 0.06[f]

[a]Reference [63].
[b]Reference [57].
[c]Reference [58].
[d]Reference [59].
[e]Reference [60].
[f]Reference [64].
[g]Reference [61].
[h]Reference [62].

TABLE III. Experimental half-lives and corresponding matrix element $M_{2\nu}$ along with the theoretically calculated $M_{2\nu}$ in different models. The numbers corresponding to (a) and (b) are calculated for $g_A=1.25$ and 1.0, respectively.

Experiment				Theory			
Reference	Projects	Half-life $T^{2\nu}_{1/2}(10^{18}$ yr)	$\lvert M_{2\nu}\rvert$	Reference	Models	$\lvert M_{2\nu}\rvert$	Half-life $T^{2\nu}_{1/2}(10^{18}$ yr)
[24]	UC Irvine	$(6.82^{+0.38}_{-0.53}\pm 0.68)$	(a) $0.125^{+0.012}_{-0.009}$		PHFB	0.143	(a) 5.18
			(b) $0.195^{+0.014}_{-0.020}$				(b) 12.7
[25]	LBL+MHC+	$(7.6^{+2.2}_{-1.4})$	(a) $0.118^{+0.013}_{-0.014}$	[31]	SSDH		(a) (8.97–7.15)
	UNM+INEL		(b) $0.185^{+0.020}_{-0.022}$	[14]	MCM		19.0
[26]	NEMO	$(9.5\pm 0.4\pm 0.9)$	(a) $0.106^{+0.008}_{-0.007}$	[32]	SRPA(WS)	0.059	(a) 30.4
			(b) $0.165^{+0.013}_{-0.010}$				(b) 74.3
[27]	LBL	(9.7 ± 4.9)	(a) $0.105^{+0.044}_{-0.020}$	[33]	SU(3)(SPH)	0.152	(a) 4.59
			(b) $0.163^{+0.069}_{-0.030}$				(b) 11.2
[28]	ELEGANTS V	$(11.5^{+3.0}_{-2.0})$	(a) $0.096^{+0.010}_{-0.010}$	[33]	SU(3)(DEF)	0.108	(a) 9.09
			(b) $0.150^{+0.015}_{-0.016}$				(b) 22.2
[29]	UC Irvine	$(11.6^{+3.4}_{-0.8})$	(a) $0.096^{+0.003}_{-0.012}$	[34]	OEM	0.054	(a) 36.4
			(b) $0.149^{+0.005}_{-0.018}$				(b) 88.8
[30]	INS Baksan	$(3.3^{+2.0}_{-1.0})$	(a) $0.179^{+0.036}_{-0.038}$	[35]	QRPA(EMP)	0.197	(a) 2.73
			(b) $0.280^{+0.055}_{-0.059}$				(b) 6.67
				[36]	QRPA(EMP)	0.256	(a) 1.62
							(b) 3.95
				[37]	QRPA		1.10
				[38]	QRPA	0.211	(a) 2.38
							(b) 5.81

To be more specific while comparing with the experimental results, we have taken the theoretical spectra to be the optimum if the excitation energy of the 2^+ state E_{2^+} is reproduced as closely as possible. In Table I, we have presented the theoretically calculated intrinsic quadrupole moments $\langle Q_0^2\rangle$ and yrast energies for the E_{2^+} to E_{6^+} levels of ^{100}Mo and ^{100}Ru for different values of χ_{pn} as experimental data are available only for these levels [56]. It is clearly observed that as the χ_{pn} is varied from -0.0178 to -0.0194 MeV b^{-4}, the intrinsic quadrupole moment $\langle Q_0^2\rangle$ increases by 7.06 units in the case of ^{100}Mo and 2.63 units in the case of ^{100}Ru. At the same time the E_{2^+} decreases by 0.384 MeV in the case of ^{100}Mo and 0.298 MeV in the case of ^{100}Ru, respectively. This observed inverse correlation between $\langle Q_0^2\rangle$ and E_{2^+}, well known from Grodzins' rule [55], is understandable as there is an enhancement in the collectivity of the intrinsic state with the increase of $|\chi_{pn}|$, hence the E_{2^+} decreases. Further, it is also noticed that the same increase of $\langle Q_0^2\rangle$ is responsible for the compression of the yrast spectra. To be more specific, the excitation energy of the 6^+ state E_{6^+} is lowered from 3.2101 to 2.4645 MeV in the case of ^{100}Mo and from 3.1337 to 2.0398 MeV in the case of ^{100}Ru as the $|\chi_{pn}|$ is increased from 0.0178 to 0.0194 MeV b^{-4}. The theoretically calculated E_{2^+} is 0.5434 MeV in comparison to the experimentally observed value 0.5355 MeV for ^{100}Mo corresponding to $\chi_{pn}=-0.0190$ MeV b^{-4}. In the case of ^{100}Ru, the observed and theoretically calculated E_{2^+} are 0.5396 and 0.5138 MeV, respectively, for $\chi_{pn}=-0.0186$ MeV b^{-4}. Thus for a given model space, SPE's G_p, G_n, and χ_{pp}, we have fixed χ_{pn} through the experimentally available energy spectra.

In Table II, we have presented the calculated as well as the experimentally observed values of the reduced transition probabilities $B(E2{:}0^+\rightarrow 2^+)$ [57–62], static quadrupole moments $Q(2^+)$ [63], and the gyromagnetic factors $g(2^+)$ [63,64]. We have given $B(E2)$ results for effective charges $e_{eff}=0.55$, 0.60, and 0.65 in columns 2 to 4, respectively. The experimentally observed values are displayed in column 5. It is noticed that the calculated values are in excellent agreement with the observed $B(E2)$ for $e_{eff}=0.60$. The theoretically calculated $Q(2^+)$ are tabulated in columns 6 to 8 for the same effective charges as given above. The experimental $Q(2^+)$ results are given in column 9. It can be seen that for the same effective charge 0.60, the agreement between the calculated and experimental values is slightly off for ^{100}Mo while in case of ^{100}Ru the calculated values differ by 6% only from the experimental limit $-0.54\pm 0.07e$ fm^2.

The $g(2^+)$ values are calculated with $g_l^\pi=1.0$, $g_l^\nu=0.0$, and $g_s^\pi=g_s^\nu=0.60$. The calculated $g(2^+)$ is 0.471 nm for ^{100}Mo and 0.357 nm for ^{100}Ru. The theoretically calculated and observed $g(2^+)$ values are in good agreement for ^{100}Mo and in case of ^{100}Ru they are off by about 0.03 nm only in the case when we consider the lower limit given by Raghavan [63]. From the overall agreement between the calculated and observed electromagnetic properties, it is clear that the PHFB wave functions of ^{100}Mo and ^{100}Ru generated by fixing χ_{pn} to reproduce the yrast spectra are quite reliable.

TABLE IV. Effect of variation in SPE of the $0h_{11/2}$ orbit on E_{2^+}, $\langle Q_0^2\rangle$, and $M_{\rm GT}^{2\nu}$.

SPE's	^{100}Mo				^{100}Ru				$M_{\rm GT}^{2\nu}$
$\epsilon(0h_{11/2})$	E_{2^+}	$\langle Q_0^2\rangle_\pi$	$\langle Q_0^2\rangle_\nu$	$\langle Q_0^2\rangle$	E_{2^+}	$\langle Q_0^2\rangle_\pi$	$\langle Q_0^2\rangle_\nu$	$\langle Q_0^2\rangle$	
8.5	0.5268	17.11	32.48	49.59	0.6100	17.53	28.28	45.82	1.7498
8.6	0.5434	16.87	32.05	48.92	0.5138	17.59	28.41	46.00	1.5721
8.7	0.5238	16.46	31.30	47.76	0.4189	17.68	28.60	46.29	1.2923
8.8	0.5191	16.20	30.74	46.94	0.3463	17.82	28.91	46.73	0.9343
8.9	0.5359	15.98	30.29	46.27	0.3240	17.90	29.08	46.98	0.7365

Hence we proceed to calculate the $M_{2\nu}$ for the $0^+\rightarrow 0^+$ transition which will provide a conclusive test regarding the reliability of the ^{100}Mo intrinsic wave function in relation to that of ^{100}Ru.

C. Results of the $2\nu\beta\beta$ decay mode

The double beta decay of $^{100}\text{Mo}\rightarrow{}^{100}\text{Ru}$ for the $0^+\rightarrow 0^+$ transition has been investigated by many experimental groups [24–30] as well as theoreticians by employing different theoretical frameworks [14,31–38]. In Table III, we have compiled all the available experimental and theoretical results along with our calculated $M_{2\nu}$ and corresponding half-life $T_{1/2}^{2\nu}$. We have used a phase space factor $G_{2\nu}=9.434\times10^{-18}$ yr^{-1} given by Doi *et al.* [8] and an energy denominator $E_d=11.2$ MeV using the relation $\langle E_N\rangle=1.12\times A^{1/2}-W_0/2$ given by Haxton and Stephenson [7]. In column 4 of Table III, we have presented the $M_{2\nu}$ extracted from the experimentally observed $T_{1/2}^{2\nu}$ using the phase space factor given above. The phase space integral has been evaluated for $g_A=1.25$ by Doi *et al.* [8]. However, in heavy nuclei it is more justified to use the nuclear matter value of g_A around 1.0. Hence, the experimental $M_{2\nu}$ as well as the theoretical $T_{1/2}^{2\nu}$ are calculated for $g_A=1.0$ and 1.25. We have presented only the theoretical $T_{1/2}^{2\nu}$ for those models for which no direct or indirect information about $M_{2\nu}$ is available to us.

In comparison to the experimental $M_{2\nu}$, the theoretically calculated values given by Stoica using SRPA(WS) [32] and Hirsh *et al.* in OEM [34] are too small. The $M_{2\nu}$ calculated by Griffiths and Vogel [36] using the QRPA model favors the results of LBL [27] and INS Baksan [30] for $g_A=1.0$ due to the large error bar in the experimental $T_{1/2}^{2\nu}$. On the other hand the $M_{2\nu}$ predicted by Suhonen and Civitarese [35] and Engel *et al.* [38] are in agreement with the results of LBL [27], the LBL Collaboration [25], and INS Baksan [30] for $g_A=1.0$. The present calculation and that of Hirsch *et al.* using SU3(SPH) [33] give nearly identical $M_{2\nu}$ values. They are close to the experimental result given by De Silva *et al.* [24] for $g_A=1.25$ while for $g_A=1.0$, the above two $M_{2\nu}$ are in agreement with the results of NEMO, LBL, ELEGANTS, and UC Irvine. Further, the value of $M_{2\nu}$ given by Hirsch *et al.* using SU3(DEF) [33] favors the results of the NEMO Collaboration [26], LBL [27], ELEGANT V [28], and UC Irvine (the results of Elliot *et al.* [29]) for $g_A=1.0$. The $2\nu\beta\beta$ decay rate of ^{100}Mo calculated by Staudt *et al.* [37] and Suhonen and Civitarese [14] are slightly off from the experimental $T_{1/2}^{2\nu}$. The results of SSDH [31] are in agreement with the experimental half-lives of UC Irvine [24], LBL [27], the LBL Collaboration [25], and the NEMO Collaboration [26].

It is clear from the above discussion that the validity of nuclear models presently employed to calculate the $M_{2\nu}$ cannot be uniquely established due to large error bars in experimental results as well as uncertainty in g_A. Further work is necessary both in the experimental as well as the theoretical front to judge the relative applicability, success, and failure of various models used so far for the study of double beta decay processes.

To understand the role of deformation on the DGT $M_{\rm GT}^{2\nu}$, we have investigated the variation of the latter with respect to the change in SPE and strength of the QQ interaction $|\chi_{qq}|$. In Table IV, we have presented the quadrupole moment of the intrinsic state $\langle Q_0^2\rangle$ and the DGT $M_{\rm GT}^{2\nu}$ for different SPE's of $0h_{11/2}$. It is observed that the $\langle Q_0^2\rangle$ decreases by 3.32 units and increases by 1.16 units in ^{100}Mo and ^{100}Ru, respectively, with the increase of $\epsilon(0h_{11/2})$ from 8.5 to 8.9 MeV. Further, the value of $M_{\rm GT}^{2\nu}$ decreases from 1.7498 to 0.7365 for the same variation in SPE of $0h_{11/2}$. It is quite clear from the above discussions that an increase in the SPE of $0h_{11/2}$ orbit produces corresponding changes in the deformation of HFB intrinsic states which results in the suppression of $M_{\rm GT}^{2\nu}$ by a factor of 2.5, approximately.

The variation of $\langle Q_0^2\rangle$ and $M_{\rm GT}^{2\nu}$ with respect to the change in χ_{qq} is presented in Table V. The $\langle Q_0^2\rangle$ of ^{100}Mo and ^{100}Ru remain almost constant as the strength of the QQ interaction is varied from 5% to 60% while the $M_{\rm GT}^{2\nu}$ increases from

TABLE V. Effect of the variation in χ_{qq} on $\langle Q_0^2\rangle$ and $M_{\rm GT}^{2\nu}$.

χ_{qq}	^{100}Mo			^{100}Ru			$M_{\rm GT}^{2\nu}$
	$\langle Q_0^2\rangle_\pi$	$\langle Q_0^2\rangle_\nu$	$\langle Q_0^2\rangle$	$\langle Q_0^2\rangle_\pi$	$\langle Q_0^2\rangle_\nu$	$\langle Q_0^2\rangle$	
0.05	0.002	0.005	0.007	0.008	0.016	0.024	1.7022
0.20	0.011	0.023	0.035	0.068	0.128	0.196	1.7931
0.40	0.040	0.086	0.126	0.037	0.083	0.119	1.8156
0.60	0.113	0.241	0.354	0.436	0.777	1.213	1.8949
0.80	1.219	2.546	3.785	5.495	8.980	14.475	2.1318
0.90	9.327	20.207	29.534	14.649	24.645	39.294	2.2815
0.95	13.786	27.885	41.671	16.414	27.109	43.523	2.1214
1.00	16.875	32.047	48.922	17.594	28.409	46.003	1.5720
1.05	18.812	34.299	53.109	18.756	29.553	48.309	1.0863
1.10	19.488	35.585	55.072	19.073	30.407	50.110	1.4215
1.20	20.438	37.392	57.830	21.419	31.802	53.221	2.4203

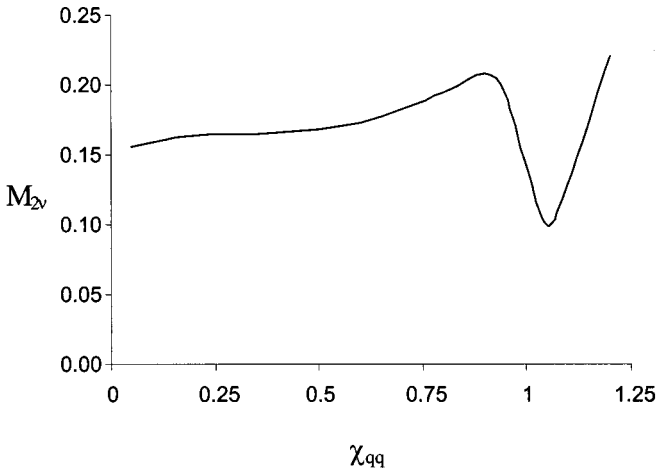

FIG. 1. The dependence of $M_{2\nu}$ on the strength of the quadrupole-quadrupole interaction χ_{qq}.

1.7022 to 1.8949. With a further rise in χ_{qq} up to 90% the $\langle Q_0^2 \rangle$ as well as the $M_{\mathrm{GT}}^{2\nu}$ increase largely. The $\langle Q_0^2 \rangle$ increases both in ^{100}Mo and ^{100}Ru and the $M_{\mathrm{GT}}^{2\nu}$ decreases to 1.0863 while the χ_{qq} is changed to 1.05. However, both the $\langle Q_0^2 \rangle$ and $M_{\mathrm{GT}}^{2\nu}$ increase monotonically as the χ_{qq} is further increased to 1.20. Thus a change of χ_{qq} triggers deformation in the HFB intrinsic states of ^{100}Mo and ^{100}Ru which is responsible for the variation of $M_{\mathrm{GT}}^{2\nu}$ by a factor of 1.5, approximately. In Fig. 1, we have displayed the dependence of $M_{2\nu}$ on the χ_{qq}. The $M_{2\nu}$ is increased as the χ_{qq} is varied from 0.05 to 0.90 and 1.05 to 1.20. It is interesting to observe that $M_{2\nu}$ decreases and gets tuned towards the realistic value as the χ_{qq} acquires a physical value around 1.0. To summarize, we have shown that the deformations of the HFB intrinsic states play an important role in reproducing a realistic $M_{\mathrm{GT}}^{2\nu}$.

IV. CONCLUSIONS

In the first step, we have tested the quality of HFB wave functions by comparing the theoretically calculated results for a number of spectroscopic properties of ^{100}Mo and ^{100}Ru nuclei with the available experimental data. To be more specific we have computed the yrast spectra, reduced $B(E2)$ transition probabilities, quadrupole moments, and g factors. Further, reliability of the intrinsic wave functions have been tested by calculating the $M_{2\nu}$. The values of $M_{2\nu}$ calculated in the PHFB model and SU3(SPH) model [33] are quite close and the calculated $2\nu\beta\beta$ decay rate $T_{1/2}^{2\nu}$ is in close agreement with the experimentally observed value of De Silva *et al.* [24] for $g_A = 1.25$. For $g_A = 1.0$ they are in agreement with the results of the NEMO Collaboration [26], LBL [27], ELEGANT V [28], and UC Irvine (the results of Elliot *et al.* [29]). Further, we have shown that the deformations of the intrinsic ground states of ^{100}Mo and ^{100}Ru play a crucial role in reproducing a realistic DGT matrix element. A reasonable agreement between the calculated and observed spectroscopic properties of ^{100}Mo and ^{100}Ru as well as the $2\nu\beta\beta$ decay rate of ^{100}Mo makes us confident to employ the same PHFB wave functions to study the $0\nu\beta\beta$ decay of ^{100}Mo which will be communicated soon.

ACKNOWLEDGMENTS

One of us (B.M.D.) would like to acknowledge the financial support provided by CTS, Indian Institute of Technology, Kharagpur, India where a part of this work was carried out.

[1] Goeppert Mayer, Phys. Rev. **48**, 512 (1935).
[2] W. Fury, Phys. Rev. **56**, 1184 (1939).
[3] E. Majorana, Nuovo Cimento **5**, 171 (1937); G. Racah, *ibid.* **4**, 322 (1937).
[4] S. L. Glashow, Nucl. Phys. **22**, 579 (1961); S. Weinberg, Phys. Rev. Lett. **19**, 1264 (1967); A. Salam, in *Elementary Particle Theory: Relativistic Groups and Analyticity*, Proceedings of the Eighth Nobel Symposium, edited by by N. Svartholm (Almqvist & Wiksells, Stokholm, 1968), p. 367.
[5] D. Bryman and C. Picciotto, Rev. Mod. Phys. **50**, 11 (1978).
[6] H. Primakoff and S. P. Rosen, Annu. Rev. Nucl. Part. Sci. **31**, 145 (1981).
[7] W. C. Haxton and G. J. Stephenson, Jr., Prog. Part. Nucl. Phys. **12**, 409 (1984).
[8] M. Doi, T. Kotani, and E. Takasugi, Prog. Theor. Phys. Suppl. **83**, 1 (1985).
[9] J. D. Vergados, Phys. Rep. **133**, 1 (1986).
[10] A. Faessler, Prog. Part. Nucl. Phys. **21**, 183 (1988).
[11] T. Tomoda, Rep. Prog. Phys. **54**, 53 (1991).
[12] F. Boehm and P. Vogel, Annu. Rev. Nucl. Part. Sci. **34**, 125 (1984); *Physics of Massive Neutrinos* (Cambridge University Press, Cambridge, England, 1987); *Physics of Neutrinos*, 2nd ed. (Cambridge University Press, Cambridge, England, 1992).
[13] M. K. Moe and P. Vogel, Annu. Rev. Nucl. Part. Sci. **44**, 247 (1994).
[14] J. Suhonen and O. Civitarese, Phys. Rep. **300**, 123 (1998).
[15] A. Faessler and F. Simkovic, hep-ph/9901215; J. Phys. G **24**, 2139 (1998).
[16] H. V. Klapdor, in *Proceedings of the International Symposium on Weak and Electromagnetic Interactions in Nuclei*, edited by H. V. Klapdor (Springer, Berlin, 1986); K. Muto and H. V. Klapdor, in *Neutrinos*, edited by H. V. Klapdor (Springer, Heidelberg, 1988); H. V. Klapdor, in *Proceedings of the International Workshop on Double Beta Decay and Related Topics*, edited by H. V. Klapdor and S. Stoica (World Scientific, Singapore, 1996); H. V. Klapdor-Kleingrothaus, hep-ex/9907040; hep-ex/9901021; hep-ex/9802007; Int. J. Mod. Phys. A **13**, 3953 (1998).
[17] L. Zhao, B. A. Brown, and W. A. Richter, Phys. Rev. C **42**, 1120 (1990).
[18] H. Nakada, T. Sebe, and K. Muto, Nucl. Phys. **A607**, 235 (1996).
[19] E. Caurier, F. Nowacki, A. Poves, and J. Retamosa, Phys. Rev. Lett. **77**, 1954 (1996).

[20] J. Suhonen, P. C. Divari, L. D. Skouras, and I. P. Johnstone, Phys. Rev. C **55**, 714 (1997).
[21] P. B. Radha, D. J. Dean, S. E. Koonin, T. T. S. Kuo, K. Langanke, A. Poves, J. Retamosa, and P. Vogel, Phys. Rev. Lett. **76**, 2642 (1996).
[22] S. E. Koonin, D. J. Dean, and K. Langanke, Phys. Rep. **278**, 1 (1997).
[23] P. Vogel and M. R. Zirnbauer, Phys. Rev. Lett. **57**, 3148 (1986).
[24] A. De Silva, M. K. Moe, M. A. Nelson, and M. A. Vient, Phys. Rev. C **56**, 2451 (1997).
[25] M. Alston-Garnjost *et al.*, Phys. Rev. C **55**, 474 (1997).
[26] NEMO Collaboration, D. Dassie *et al.*, Phys. Rev. D **51**, 2090 (1995).
[27] A. Garcia *et al.*, Phys. Rev. C **47**, 2910 (1993).
[28] H. Ejiri *et al.*, J. Phys. G **17**, 155 (1991); Nucl. Phys. **A611**, 85 (1996).
[29] S. R. Elliott, M. K. Moe, M. A. Nelson, and M. A. Vient, J. Phys. G **17**, S145 (1991).
[30] S. I. Vasilev *et al.*, Pis'ma Zh. Éksp. Teor. Fiz. **51**, 550 (1990) [JETP Lett. **51**, 622 (1990)]; **58**, 177 (1993) [**58**, 178 (1993)].
[31] F. Simkovic, P. Domin, and S. V. Semenov, nucl-th/0006084.
[32] S. Stoica, Phys. Lett. B **350**, 152 (1995).
[33] J. G. Hirsch, O. Castanos, P. O. Hess, and O. Civitarese, Phys. Rev. C **51**, 2252 (1995).
[34] M. Hirsch *et al.* Z. Phys. A **347**, 151 (1994).
[35] J. Suhonen and O. Civitarese, Phys. Rev. C **49**, 3055 (1994).
[36] A. Griffiths and P. Vogel, Phys. Rev. C **46**, 181 (1992).
[37] A. Staudt, K. Muto, and H. V. Klapdor, Europhys. Lett. **13**, 31 (1990).
[38] J. Engel, P. Vogel, and M. R. Zirnbauer, Phys. Rev. C **37**, 731 (1988).
[39] E. Cheifetz *et al.*, Phys. Rev. Lett. **25**, 38 (1970).
[40] L. D. Skouras and J. D. Vergados, Phys. Rev. C **28**, 2122 (1983); K. Grotz, H. V. Klapdor, and J. Metzinger, J. Phys. G **9**, L169 (1983).
[41] T. Tsuboi, K. Muto, and H. Horie, Phys. Lett. **143B**, 293 (1984).
[42] S. K. Khosa, P. N. Tripathi, and S. K. Sharma, Phys. Lett. **119B**, 257 (1982).
[43] P. N. Tripathi, S. K. Sharma, and S. K. Khosa, Phys. Rev. C **29**, 1951 (1984).
[44] S. K. Sharma, P. N. Tripathi, and S. K. Khosa, Phys. Rev. C **38**, 2935 (1988).
[45] P. K. Rath and S. K. Sharma, Phys. Rev. C **38**, 2928 (1988).
[46] S. K. Sharma, G. Mukherjee, and P. K. Rath, Phys. Rev. C **41**, 1315 (1990).
[47] A. L. Goodman, in *Advances in Nuclear Physics*, edited by J.W. Negele and E. Voget (Plenum, New York, 1979), Vol. 11, p. 263.
[48] N. Onishi and S. Yoshida, Nucl. Phys. **80**, 367 (1966).
[49] J. D. Vergados and T. T. S. Kuo, Phys. Lett. **35B**, 93 (1971).
[50] P. Federman and S. Pittel, Phys. Lett. **77B**, 29 (1978).
[51] M. Baranger and K. Kumar, Nucl. Phys. **A110**, 490 (1968).
[52] G. M. Heestand, R. R. Borchers, B. Herskind, L. Grodzins, R. Kalish, and D. E. Murnick, Nucl. Phys. **A133**, 310 (1969).
[53] W. Greiner, Nucl. Phys. **80**, 417 (1966).
[54] A. Arima, Nucl. Phys. **A354**, 19 (1981).
[55] L. Grodzins, Phys. Lett. **2**, 88 (1962).
[56] M. Sakai, At. Data Nucl. Data Tables **31**, 400 (1984).
[57] H. Bhon, P. Kienle, D. Proetel, and R. L. Hershberger, Z. Phys. A **274**, 327 (1975).
[58] P. Paradis, G. Lamoureux, R. Lecomte, and S. Monaro, Phys. Rev. C **14**, 835 (1976).
[59] B. Singh and J. A. Szucs, Nucl. Data Sheets **60**, 1 (1990).
[60] S. Raman, C. W. Nestor, Jr., S. Kahane, and K. H. Bhatt, At. Data Nucl. Data Tables **36**, 1 (1987).
[61] B. J. Lieb, H. S. Plendl, H. O. Funsten, C. E. Stronach, and V. G. Lind, Phys. Rev. C **22**, 1612 (1980).
[62] J. H. Hirata and O. Dietzsch, Proceedings of the International Conference on Nuclear Physics, Berkeley, 1980, p. 102.
[63] P. Raghavan, At. Data Nucl. Data Tables **42**, 189 (1989).
[64] A. Giannatiempo, A. Nannini, P. Sona, and D. Cutoiu, Phys. Rev. C **52**, 2969 (1995).